IEEE Photonics Journal
An IEEE Photonics Society Publication

Advanced Chromatic Dispersion Compensation in Optical Fiber FBMC-OQAM Systems

Volume 9, Number 6, December 2017

Francois Rottenberg
Trung-Hien Nguyen
Simon-Pierre Gorza
Francois Horlin
Jerome Louveaux

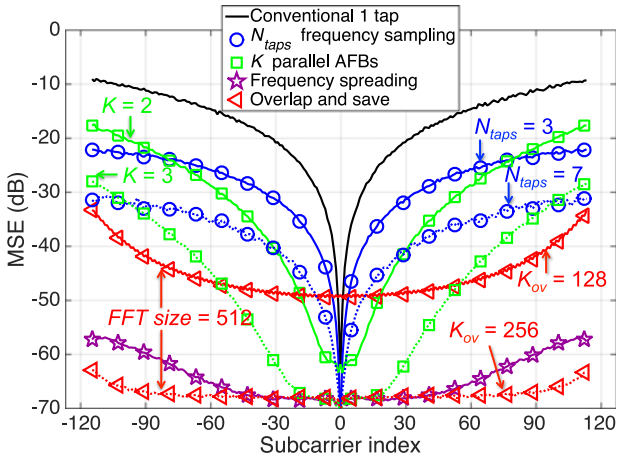

DOI: 10.1109/JPHOT.2017.2773667
1943-0655 © 2017 IEEE

Advanced Chromatic Dispersion Compensation in Optical Fiber FBMC-OQAM Systems

Francois Rottenberg,[1,2] **Trung-Hien Nguyen**,[2]
Simon-Pierre Gorza,[2] **Francois Horlin**,[2] **and Jerome Louveaux**[1]

[1]ICTEAM Institute, Université catholique de Louvain, 1348 Louvain-la-Neuve, Belgium
[2]OPERA Department, Université libre de Bruxelles, 1050 Brussels, Belgium

DOI:10.1109/JPHOT.2017.2773667

Manuscript received September 25, 2017; revised November 9, 2017; accepted November 10, 2017. Date of publication November 22, 2017; date of current version November 30, 2017. This research was supported in part by Fonds pour la Formation a la Recherche dans l'Industrie et dans l'Agriculture and in part by Belgian Fonds National de la Recherche Scientifique (FNRS) under Grant PDR T.1039.15.
Corresponding author: Francois Rottenberg (e-mail: francois.rottenberg@uclouvain.be).

Abstract: We report on several methods for the chromatic dispersion (CD) compensation in optical fiber offset-QAM-based filterbank multicarrier (FBMC-OQAM) systems. We show that several equalization structures, initially proposed for wireless FBMC-OQAM systems, can also be applied to optical FBMC-OQAM systems to enhance the CD tolerance. The different CD compensation algorithms are numerically validated and compared to the conventional one tap equalizer in a 30-Gbaud optical FBMC system, in terms of performance and complexity. Considering a 1-dB optical signal-to-noise ratio penalty at a bit error rate of 3.8×10^{-3} and 256 subcarriers, the results show that the maximum CD tolerance of the frequency spreading method can be enhanced by a factor 10 and 30 for 4-OQAM and 16-OQAM modulations, respectively, compared to that of the conventional one-tap equalizer, at the cost of higher complexity. Even though the other CD compensation methods provide a reduced CD tolerance compared to the frequency spreading method, they require less complexity and hence can be good alternatives.

Index Terms: FBMC-OQAM, optical fiber, coherent communication, chromatic dispersion (CD).

1. Introduction

Offset-QAM-based filterbank multicarrier (FBMC-OQAM) has been recently proposed in optical fiber communication systems [1]–[3]. FBMC-OQAM modulations use a pulse shape which is well localized in time and frequency, making the system more robust against time and frequency variations of the channel [4]. The main advantage of FBMC-OQAM for optical fiber communications is its increased spectral efficiency (SE). Thanks to the very low spectral leakage of its prototype filter, it is sufficient to insert a very small guard band of one or two subcarriers between unsynchronized lasers, which results in a higher SE [3]. Moreover, as opposed to orthogonal frequency division multiplexing modulation (OFDM), FBMC-OQAM does not require the use of a cyclic prefix, which again increases its SE.

Chromatic dispersion (CD) is one of the main transmission impairments in optical fiber systems. It is due to the fact that spectral components of the transmitted signal travel at different speeds

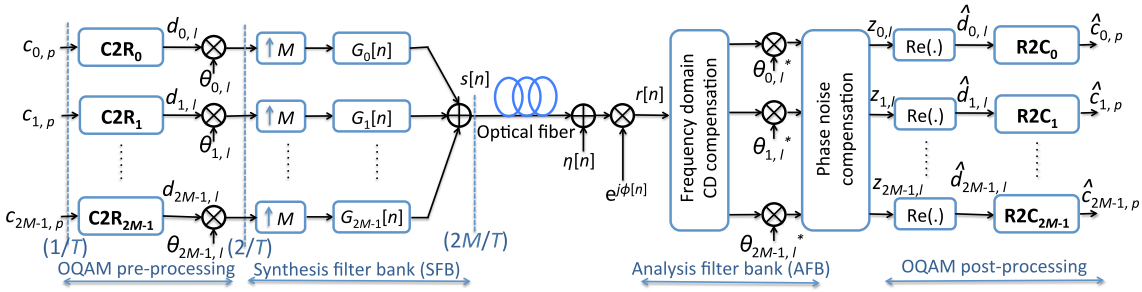

Fig. 1. FBMC-OQAM optical transmission model for considering the chromatic dispersion impact.

inside the fiber. The classical way to handle channel frequency variations in FBMC-OQAM systems is to increase the number of subcarriers, so that the channel can be approximated as flat at the subcarrier level. Then, simple one-tap equalization can be used, providing an efficient replacement of the well-known overlap and save algorithm [1]. However, for a fixed bandwidth, having more subcarriers induces a larger symbol period and hence, more sensitivity to phase noise (PN) [2].

In this paper, we consider a system with a sufficiently high number of subcarriers such that it can achieve high SE. At the same time, we keep the number of subcarriers low enough such that the system remains robust against PN. In that case, and for relatively long fibers, simple one-tap equalization is not sufficient and more advanced CD compensation methods are necessary [1], [5], [6]. Here, we review several compensation algorithms and we show that these methods, initially designed to handle channel frequency selectivity in wireless systems, can be applied to optical fiber communications. The different algorithms are compared in terms of performance and complexity.

2. System Model

In order to focus on the CD effect and its compensation methods, an FBMC-OQAM transmission with only one polarization is considered, as depicted in Fig. 1. Dual polarization systems can straightforwardly be achieved by using some existing techniques in OFDM systems for both polarization multiplexing and demultiplexing [7]. Ideal time/frequency synchronization is assumed. The number of subcarriers, subcarrier index and QAM symbol duration are denoted by $2M$, m and T, respectively. At the transmitter, the real-valued transmitted symbols $d_{m,l}$ are obtained after de-staggering of the complex-valued QAM symbols $c_{m,l}$ ($\mathbf{C2R}_m$). The symbols $d_{m,l}$ are FBMC-OQAM modulated using a prototype pulse $g[n]$ of length $L_g = 2M\kappa$ where κ is the overlapping factor, with energy normalized to one and with near perfect reconstruction properties [8]. In practice, the synthesis filter bank (SFB) and analysis filter bank (AFB) are efficiently implemented through the combination of a polyphase network (PPN) and a fast Fourier transform (FFT) [9]. The transmitted signal $s[n] \in \mathbb{C}$ can be written as

$$s[n] = \sum_{l=-\infty}^{+\infty} \sum_{m=0}^{2M-1} d_{m,l}\,\theta_{m,l}\,g_{m,l}[n] \tag{1}$$

where $\theta_{m,l} = j^{l+m}$ and $g_{m,l}[n] = g[n - lM]\,e^{j\frac{2\pi}{2M}m\left(n-lM-\frac{L_g-1}{2}\right)}$. The phase term $\frac{L_g-1}{2}$ is inserted in order to have a causal filter $g_{m,l}[n]$ [9]. A The CD is assumed to have the following baseband frequency response

$$H(f) = e^{-j\frac{\pi D\lambda^2 L}{c}f^2} \tag{2}$$

where D is the dispersion parameter [ps/nm/km], λ is the central wavelength, c is the speed of light and L is the fiber length [10]. The received signal, impacted by CD, PN and additive noise, can be

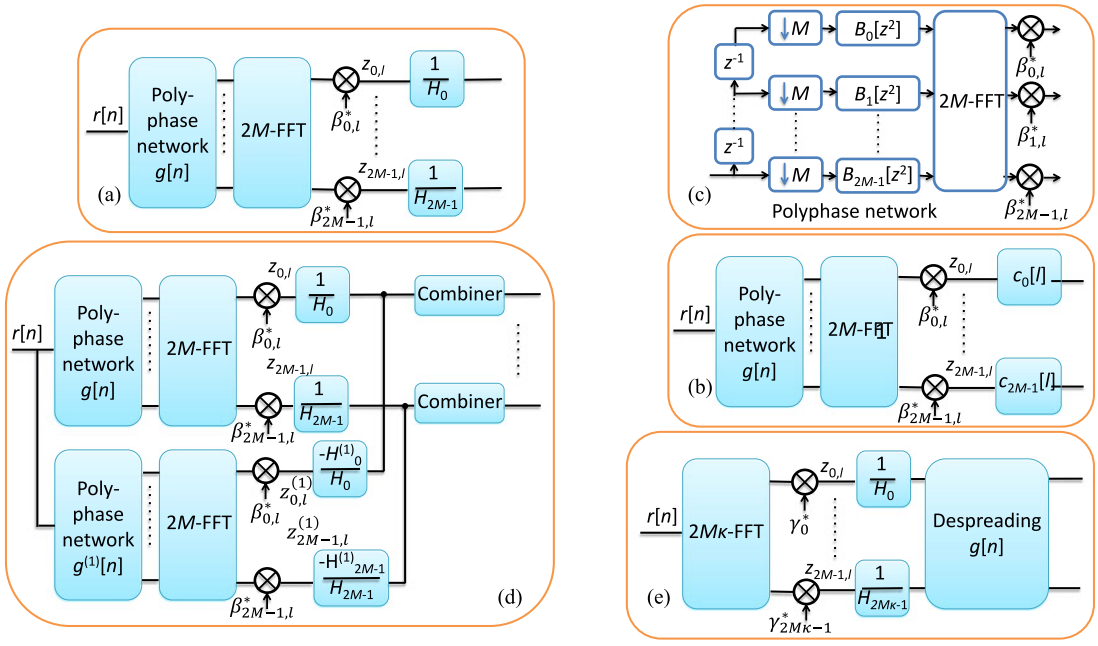

Fig. 2. Equalizer structures for chromatic dispersion compensation: (a) 1-tap equalizer; (b) Polyphase network structure, where $B_m(z^2)$ is the two times upsampled m-th polyphase component of the prototype filter $g[n]$ and $\beta_{m,l} = (-1)^{ml} e^{-j\frac{2\pi}{2M} m \frac{L_g-1}{2}}$; (c) Multi-tap fractionally spaced per-subcarrier equalizer; (d) Parallel multi-stage equalizer where $\gamma_m = e^{-j\frac{2\pi}{2M_K} m \frac{L_g-1}{2}}$; (e) Frequency spreading equalizer.

written as

$$r[n] = \left(\int_{-1/2T_s}^{1/2T_s} S(f)\, H(f)\, e^{j2\pi f T_s n} df + w[n] \right) e^{j\phi[n]} \tag{3}$$

where $S(f)$ is the Fourier transform of the transmitted signal, $T_s = \frac{T}{2M}$ is the sampling period and the samples $w[n]$ are additive circularly-symmetric white Gaussian noise samples with zero mean and variance σ_w^2. The additive noise represents the amplified spontaneous noise (ASE) of optical amplifiers together with thermal and shot noises. The combined PN of linewidth $\Delta\nu$ coming from transmitter and receiver lasers is modeled as a Wiener process $\phi[n] = \phi[n-1] + \psi[n]$, where $\psi[n]$ is a zero mean real Gaussian random variable with variance $\sigma_\psi^2 = \pi \Delta\nu T/M$. At the receiver, the signal after demodulation, at subcarrier m_0 and multicarrier symbol l_0, denoted by z_{m_0,l_0}, is given by

$$z_{m_0,l_0} = \sum_{n=0}^{L_g-1} r[n]\, g^*_{m_0,l_0}[n]. \tag{4}$$

In classical approaches of FBMC-OQAM transmissions, the channel is assumed to be frequency flat at the subcarrier level and the phase noise is assumed to slowly vary with respect to the symbol duration. Under these conditions and if the pulse $g[n]$ is well localized in time and frequency, an approximation of z_{m_0,l_0} is given by (neglecting additive noise)

$$z_{m_0,l_0} \approx e^{j\phi_{l_0}} H_{m_0} \sum_{l=-\infty}^{+\infty} \sum_{m=0}^{2M-1} d_{m,l}\theta_{m,l} \sum_{n=0}^{L_g-1} g_{m,l}[n]\, g^*_{m_0,l_0}[n] \tag{5}$$

where $H_m = H(f_m)$ with f_m being the frequency of subcarrier m. As shown in Fig. 2(a), CD equalization is performed by a simple one-tap multiplication after the PPN (Fig. 2(b)) and the FFT operations. Assuming that the PN $\hat{\phi}_{l_0}$ is estimated and compensated after the CD compensation, i.e. [11], and

using the fact that $\Re\left\{\theta_{m,l}\theta^*_{m_0,l_0}\sum_{n=0}^{L_g-1} g_{m,l}[n]\, g^*_{m_0,l_0}[n]\right\} = \delta_{m-m_0,l-l_0}$, where $\Re$ is the real part operator, the transmitted symbols can be recovered by taking the real part

$$\hat{d}_{m_0,l_0} = \Re\left\{\frac{z_{m_0,l_0}\theta^*_{m_0,l_0}e^{-j\hat{\phi}_{l_0}}}{H_{m_0}}\right\}. \tag{6}$$

The quality of the detection will critically depend on the accuracy of the approximation in (5) [12]. For long fibers, the channel will exhibit fast phase variations, especially at the edges of the band [6], which can be seen as a highly selective channel. To counterbalance this effect and to improve the accuracy of (5), one could decrease the subcarrier spacing $1/T$. This can be achieved by increasing the number of subcarriers in the system, while the transmission bandwidth, $1/T_s$, remains fixed. However, increasing the number of subcarriers also means an increased symbol period $T = 2MT_s$, making the system more sensitive to time variations of the channel and hence to PN. In other words, more advanced equalization techniques should be analyzed to compensate for CD, especially for long communication links and for a relatively low number of subcarriers.

3. Equalization Algorithms for Chromatic Dispersion Compensation

In this section, we describe several equalization algorithms for the CD compensation. Except for the overlap and save algorithm [1], the other techniques were initially proposed for wireless FBMC-OQAM communications under high channel frequency selectivity and can be adapted straightforwardly to FBMC-OQAM communications on optical fiber to compensate for CD.

3.1 Overlap and Save

This method, widely applied in single-carrier and multi-carrier optical fiber communication systems, convolves the received signal with an equalization filter, whose impulse response is designed to invert the effect of CD. Classically, this filtering operation is implemented in an efficient manner using the overlap and save algorithm. The algorithm first takes an FFT of block of size N on the received signal, the FFT outputs are then multiplied by the inverse of the CD frequency response and brought back to time domain by inverse FFT (IFFT) of size N. Finally, $K_{ov}/2$ samples are discarded at the beginning and at the end of the block, which yields a block of $N - K_{ov}$ samples, assumed to be approximately free from CD. These samples are then fed to the AFB [1]. Note that the parameters N and K_{ov} do not need to be related to the number of subcarriers $2M$ and that the overlap and save algorithm adds a delay of NT_s seconds to the demodulation chain.

3.2 Multi-Tap Fractionally Spaced Per-Subcarrier Equalizer

A well-known equalization approach is the multi-tap per-subcarrier equalizer [13]–[15], as shown in Fig. 2(c). Even if the outputs of the adjacent subcarriers are not used, the fractional spacing $T/2$ of the equalizer allows for efficient mitigation of inter-symbol interference (ISI) and inter-channel interference (ICI), provided that the roll-off factor of the pulse is smaller than or equal to one, as it is commonly the case in FBMC-OQAM systems [8]. The equalized symbol at the receiver can be written as

$$\hat{d}_{m_0,l_0} = \Re\left\{e^{-j\hat{\phi}_{l_0}}\theta^*_{m_0,l_0}\sum_{l=0}^{N_{taps}-1} c_{m_0}[l]\, z_{m_0,l_0-l+\alpha}\right\} \tag{7}$$

where α is introduced in order to take into account the reconstruction delay and N_{taps} is the number of taps of the equalizer. One advantage of this algorithm for optical fiber communication is its flexibility, since the deployment of the equalizer can be restricted to critical subcarriers, i.e. the subcarriers on the edges. Note that the equalizer adds a delay of $(N_{taps}-1)T/2$ seconds in the demodulation process. In the following, we describe two ways of computing the coefficients of the equalizer $c_{m_0}[l]$.

3.2.1 Minimum Mean Squared Error Equalizer: The minimum mean squared error (MMSE) equalizer [13], [15] optimizes the coefficients $c_{m_0}[l]$ in order to minimize the mean squared error of the symbol estimate. This requires to evaluate, for each subcarrier, the equivalent channel made up of the convolution of the transmit filters, the channel and the receive filters, taking into account the interference of the two adjacent subcarriers.

3.2.2 Frequency Sampling Equalizer: The principle of the frequency sampling technique is to choose certain values for the equalizer coefficients so that the equalizer frequency response is forced to pass through some target frequency points in the subchannel of interest [13], [14]. The target frequency points are chosen according to a zero forcing (ZF) or MMSE criterion. If the channel is not too selective in frequency, one can expect the equalizer response to approximate well the optimal ZF or MMSE frequency response. This design allows for a simpler computation of the equalizer coefficients. Given that the amplitude of the CD response is constant over frequency, there is no large gain of using the MMSE criterion rather than the ZF one for the target frequency points. In the evaluation of the system performance in Section 5, we will focus on the frequency sampling implementation of the multi-tap fractionally spaced per-subcarrier equalizer.

3.3 Parallel Multi-Stage Equalizer

This equalization structure was initially proposed in [16]. This receiver uses K AFB's working in parallel on the received signal, as depicted in Fig. 2(d) for the special case $K = 2$. The $k-$th AFB is using the $k-$th derivative of the prototype pulse with respect to time. The demodulated symbols coming from the $k-$th parallel AFB, denoted by $z^{(k)}_{m_0,l_0}$, are then equalized by the $k-$th derivative of the equalizer with respect to frequency. Finally, the outputs of each AFB are re-combined in order to cancel the K first orders of the distortion caused by the channel variations and the symbol is estimated as

$$\hat{d}_{m_0,l_0} = \Re\left\{ e^{-j\hat{\phi}_{l_0}} \theta^*_{m_0,l_0} \sum_{k=0}^{K-1} \frac{j^k \left(H^{-1}_{m_0}\right)^{(k)}}{(2M)^k} z^{(k)}_{m_0,l_0} \right\} \tag{8}$$

where $\left(H^{-1}_{m_0}\right)^{(k)}$ denotes the $k-$th derivative of the inverse of the channel frequency response evaluated at subcarrier m_0. Note that this processing does not require any additional delay as opposed to multi-tap equalizers.

3.4 Frequency-Spreading Receiver

Several recent works have looked at an alternative scheme to implement FBMC systems, which is the so-called frequency-spreading FBMC (FS-FBMC) technique [17], [18]. It can be seen as a special case of the fast-convolution implementation of FBMC [19]. In the FS-FBMC implementation of the receiver, an FFT of size $2M\kappa$ is first taken on the received signal, as shown in Fig. 2(e). Then, the output bins of the FFT are equalized to compensate for CD before being re-combined by the prototype pulse coefficients in the frequency domain ("de-spreading"). Finally, the real part of the symbols after the PN compensation is taken to estimate the transmitted symbols. The complexity of FS-FBMC is larger than the classical structure relying on a PPN, due to the increased FFT size. However, the advantage of the approach comes from its simplicity of understanding and from the very efficient channel equalization being done in the frequency domain at the high resolution $1/2M\kappa$ and without additional delay.

4. Complexity Comparison

First note that since the CD effect is assumed to be static over time, the equalizer coefficients should be computed only once and for all at the beginning of the transmission or off-line. Therefore we omitted this type of complexity in the comparison.

TABLE 1
Complexity of Implementation of the Algorithms

Equalization structure	**Real − valuedmultiplications**
Single-tap, per-subcarrier	$2M\ (\log_2(2M) + 2\kappa + 1) + 4$
Multi-tap, per-subcarrier	$2M\ (\log_2(2M) + 2\kappa + 4N_{\text{taps}} - 3) + 4$
Parallel multi-stage	$(2M\ (\log_2(2M) + 2\kappa + 1) + 4)\,K$
Frequency spreading	$2M\kappa\,(\log_2(2M\kappa) + 5) - 8M\ + 4$
Overlap and save	$\frac{M}{N-K_{ov}}\,(2N\log_2(N) - 2N + 8) + 2M\ (\log_2(2M) + 2\kappa - 3) + 4$

TABLE 2
Equalizers Complexity for the Considered Parameters: $2M = 256$ and $\kappa = 4$

Equalization structure	**Real − valuedmultiplications**
Single-tap, per-subcarrier	4356
Multi-tap, per-subcarrier	$N_{\text{taps}} = 3 \rightarrow 6404, \quad N_{\text{taps}} = 7 \rightarrow 10500$
Parallel multi-stage	$K = 2 \rightarrow 8712, \quad K = 3 \rightarrow 13068$
Frequency spreading	14340
Overlap and save	$N = 512, \quad K_{ov} = 128 \rightarrow 6065$ $N = 512, \quad K_{ov} = 256 \rightarrow 7432$ $N = 1024, \quad K_{ov} = 512 \rightarrow 7942$

In Table 1, the complexity of implementation of the different algorithms, in terms of real-valued multiplications, is compared. For the calculation, we assume that the number of subcarriers is a power of two and that an FFT/IFFT of size $2M$ requires $2M\,(\log_2(2\text{M}) - 3) + 4$ real-valued multiplications using the split-radix algorithm [20]. The classical receiver using single-tap per-subcarrier equalization, as described in Section 2, can be efficiently implemented using a $2M-$ FFT, a PPN and a single-tap per-subcarrier equalizer. The multi-tap fractionally spaced per-subcarrier equalizer has an increased complexity due to the additional filtering by a $N_{\text{taps}}-$ equalizer. The parallel multi-stage structure has a complexity that simply scales linearly with the number of parallel AFB's K. The frequency-spreading receiver uses a FFT of size $2M\kappa$. Each bin of the FFT is equalized and filtered to retrieve the transmitted symbol. Finally, the overlap and save algorithm is composed of an FFT of size N, N complex multiplications and another IFFT of size N, followed by one AFB. The penalty due to the K_{ov} discarded samples was also taken into account. Table 2 gives the complexity of the different CD equalization methods when the number of subcarriers is 256 and the Phydyas prototype filter with overlapping factor equal to 4 is used [8].

5. Numerical Results

In order to evaluate the effectiveness of the proposed CD compensation methods, a 30-GBaud FBMC system is simulated and 4- and 16-OQAM modulations are considered. The combined linewidth of the transmitter and receiver lasers is set to 200 kHz, which is a typical value of the commercial external cavity laser. The adaptive maximum likelihood algorithm presented in [11] is

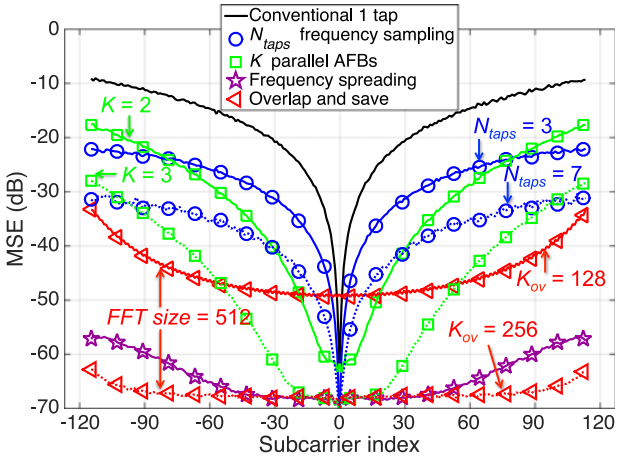

Fig. 3. MSE of symbols versus subcarrier index.

used for compensation of the PN after CD equalization. Since the number of subcarriers $2M = 256$ shows a good compromise between the CD and PN compensation [11], it is chosen for the following investigation. Ten percents of the subcarriers at the edges of the band and the center (DC) subcarrier remain inactive.

First, additive noise is not included in the simulations. This allows to clearly identify the impact of CD on the system performance. Fig. 3 shows the mean square error (MSE) of received symbols for each subcarrier after a 1000 km optical fiber transmission using different CD compensation methods. The dispersion coefficient D of standard single-mode fiber (SSMF) used in simulations is chosen equal to 17 ps/nm/km. It can be seen that the MSE exhibits the highest values on the edges of the frequency band since the phase variations of the channel are increasing with the absolute value of frequency. As it would be expected, the MSE reduces when applying the CD compensation methods. The performance is improved by increasing the block size of the overlap and save method, the number of taps of the fractionally-spaced per-subcarrier equalizer, the number of parallel AFBs equalizer, at the cost of increasing the receiver complexity. The high CD tolerance of the frequency spreading structure comes from the efficient equalization being performed at the very high frequency resolution $1/2M\kappa$. A basic assumption of the parallel equalization structure is that the derivatives of the channel frequency response should remain bounded [16], which becomes less accurate at the edges of the band and explain the performance degradation for these subcarriers. The frequency sampling multi-tap equalizer does not suffer from this limitation and outperforms the parallel equalization structure at the spectrum edges while performing relatively worse in the center frequencies.

In the next step, the FBMC system under the impact of CD is investigated in the presence of additive noise. The commonly used optical signal-to-noise ratio (OSNR) can be linked to the SNR per bit SNR_b used in wireless communications by [21]

$$OSNR = \frac{R_b}{2B_{ref}} SNR_b \tag{9}$$

where R_b is the information bit rate and B_{ref} is the reference bandwidth, which is commonly 12.5 GHz corresponding to a 0.1 nm resolution bandwidth of optical spectrum analyzers at 1550 nm carrier wavelength. Fig. 4(a) and (b) present the bit-error-ratio (BER) as a function of the OSNR after a 1000 km optical fiber transmission for 4- and 16-OQAM modulations, respectively. Considering the BER of 3.8×10^{-3} as the soft forward error correction (FEC) limit [22], the conventional 1 tap equalizer is not sufficient to compensate for the CD induced by 1000 km fiber transmission for both modulation formats. By applying the proposed CD compensation methods, the OSNR penalties of the CD compensation curves compared to that of back-to-back (B2B, no transmission) curve

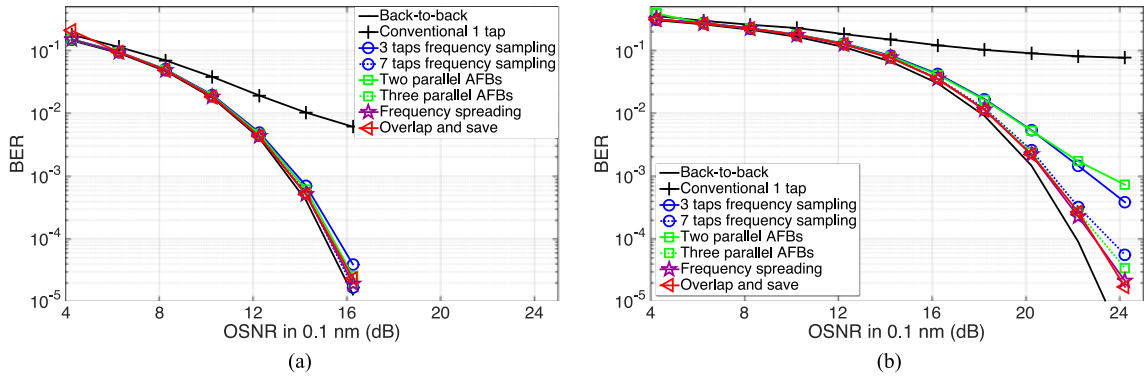

Fig. 4. BER versus OSNR for (a) 4-OQAM and (b) 16-OQAM modulations.

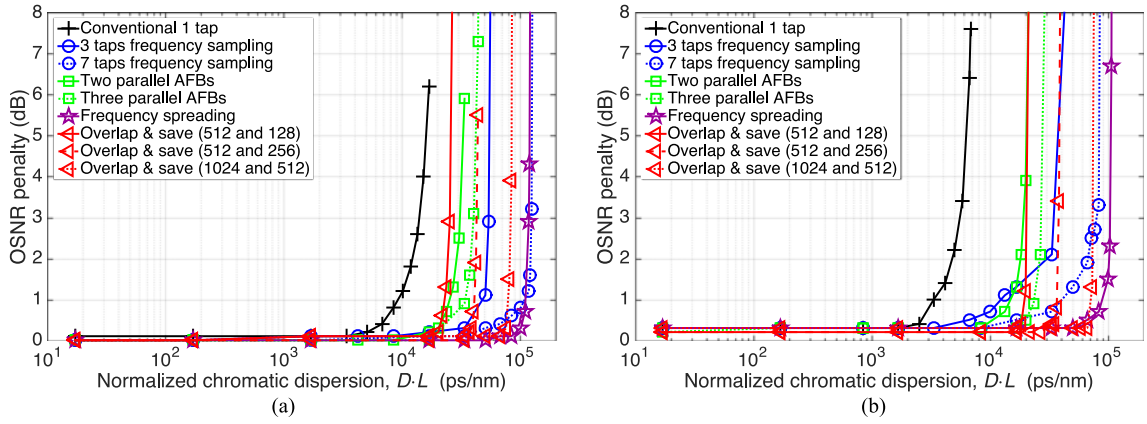

Fig. 5. OSNR penalty as a function of the normalized CD for (a) 4-OQAM and (b) 16-OQAM modulations.

at the 3.8×10^{-3} BER are negligible for 4-OQAM modulations (Fig. 4(a)). However, for 16-OQAM modulations (Fig. 4(b)), the CD compensation by using the 3 tap frequency sampling equalizer and the two parallel-AFBs equalizer are less effective than the other CD compensations. More specifically, at the soft FEC limit, the former CD compensations exhibit about 2 dB OSNR penalty whereas the latter CD compensations present only about 0.3 dB OSNR penalty compared to the B2B level.

Finally, the OSNR penalty at the 3.8×10^{-3} BER as a function of the normalized CD using different CD compensation methods is shown in Fig. 5(a) and (b) for 4- and 16-OQAM modulations, respectively. The normalized CD is defined as the product of the dispersion coefficient and the fiber length, i.e., DL [ps/nm]. Considering a 1-dB OSNR penalty and 4-OQAM modulations (Fig. 5(a)), the tolerated CD of the conventional 1 tap equalizer is only 9×10^3 ps/nm. The tolerated CD of the 3 taps and 7 taps frequency sampling equalizers are increased to 5×10^4 ps/nm and 1.1×10^5 ps/nm, respectively. Whereas the two and three parallel-AFBs equalizers show the corresponding tolerated CD of 2.5×10^4 ps/nm and 3.5×10^4 ps/nm. The frequency spreading method can provide the tolerated CD as high as the 7 taps frequency sampling equalizer, however, at the cost of higher complexity (Table 2). The tolerated CD of the overlap-and-save method can vary by adjusting the FFT size and overlapping factor. For example, when the FFT size and overlapping factor are 1024 and 512, respectively, the tolerated CD is 8×10^4 ps/nm. Similar to the other methods, the tolerated CD can be increased at the price of increasing the complexity. For 16-OQAM modulations (Fig. 5(b)), the similar tendencies are observed for different CD compensation methods, however, the tolerated CD is reduced compared to the case of 4-OQAM modulations. It is worth noticing that the frequency sampling equalizer seems to be more sensitive to higher modulation formats

than the other methods. More particularly, at the 1-dB OSNR penalty, the tolerated CD of the 3 taps frequency sampling equalizer is reduced to that of the two parallel-AFBs equalizer. While the tolerated CD of the 7 taps frequency sampling equalizer is no longer similar to that of the frequency spreading equalizer, as in 4-OQAM modulations case. Note that, although a varying number of subcarriers is not studied here, it is pointed out in [5] that the CD tolerance can scale linearly with the increase of the number of subcarriers. However, the PN compensation algorithm may become the main limitation of the system if the number of subcarriers is too large, which would require more efficient PN algorithms.

6. Conclusions

We investigated the compensation of CD in optical fiber FBMC-OQAM systems. It was shown that several equalization structures, initially proposed for wireless systems, can be applied to optical FBMC-OQAM systems even when the number of subcarriers is moderate. This allows for simple PN compensation methods working in the frequency domain. The various algorithms propose different trade-off between performance and complexity of implementation. The frequency spreading and parallel multi-stage architectures do not add any delay to the demodulation chain as opposed to the overlap and save and the multi-tap equalizers. The frequency spreading receiver and certain versions of the overlap and save algorithms showed very high robustness to CD. The disadvantage of the frequency spreading is its implementation complexity. The multi-tap equalizer is flexible in the sense that it can be applied on a subcarrier-basis depending on the CD frequency response.

Acknowledgment

The authors wish to thank the anonymous reviewers for their valuable suggestions.

References

[1] J. Fickers, A. Ghazisaeidi, M. Salsi, G. Charlet, P. Emplit, and F. Horlin, "Multicarrier offset-QAM for long-haul coherent optical communications," *J. Lightw. Technol.*, vol. 32, no. 24, pp. 4671–4678, Dec. 2014.
[2] T. H. Nguyen, J. Louveaux, S. P. Gorza, and F. Horlin, "Simple feedforward carrier phase estimation for optical FBMC/OQAM systems," *IEEE Photon. Technol. Lett.*, vol. 28, no. 24, pp. 2823–2826, Dec. 2016.
[3] Z. Li *et al.*, "Experimental demonstration of 110-Gb/s unsynchronized band-multiplexed superchannel coherent optical OFDM/OQAM system," *Opt. Express*, vol. 21, no. 19, pp. 21924–21931, 2013.
[4] B. Farhang-Boroujeny, "OFDM versus filter bank multicarrier," *IEEE Signal Process. Mag.*, vol. 28, no. 3, pp. 92–112, May 2011.
[5] J. Zhao and P. D. Townsend, "Dispersion tolerance enhancement using an improved offset-QAM OFDM scheme," *Opt. Express*, vol. 23, no. 13, pp. 17638–17652, Jun. 2015.
[6] Y. Yu, P. D. Townsend, and J. Zhao, "Equalization of dispersion-induced crosstalk in optical offset-QAM OFDM systems," *IEEE Photon. Technol. Lett.*, vol. 28, no. 7, pp. 782–785, Apr. 2016.
[7] X. Liu and F. Buchali, "Intra-symbol frequency-domain averaging based channel estimation for coherent optical OFDM," *Opt. Express*, vol. 16, no. 26, pp. 21944–21957, Dec 2008. [Online]. Available: http://www.opticsexpress.org/abstract.cfm?URI=oe-16-26-21944
[8] M. G. Bellanger, "Specification and design of a prototype filter for filter bank based multicarrier transmission," in *Proc. IEEE Int. Conf. Acoust., Speech, Signal Process.*, 2001, pp. 2417–2420.
[9] P. Siohan, C. Siclet, and N. Lacaille, "Analysis and design of OFDM/OQAM systems based on filterbank theory," *IEEE Trans. Signal Process.*, vol. 50, no. 5, pp. 1170–1183, May 2002.
[10] S. J. Savory, "Digital filters for coherent optical receivers," *Opt. Express*, vol. 16, no. 2, pp. 804–817, Jan. 2008.
[11] T. H. Nguyen, F. Rottenberg, S. P. Gorza, J. Louveaux, and F. Horlin, "Efficient chromatic dispersion compensation and carrier phase tracking for optical fiber FBMC/OQAM systems," *J. Lightw. Technol.*, vol. 35, no. 14, pp. 2909–2916, Jul. 2017.
[12] F. Rottenberg, X. Mestre, D. Petrov, F. Horlin, and J. Louveaux, "Parallel equalization structure for MIMO FBMC-OQAM systems under strong time and frequency selectivity," *IEEE Trans. Signal Process.*, vol. 65, no. 17, pp. 4454–4467, Sep. 2017.
[13] J. Louveaux *et al.*, "Equalization and demodulation in the receiver (single antenna)," PHYDYAS, Tech. Rep. ICT-211887, July 2008. [Online]. Available: http://www.ict-phydyas.org/delivrables/PHYDYAS-D3.1.pdf/view
[14] T. Ihalainen, T. H. Stitz, M. Rinne, and M. Renfors, "Channel equalization in filter bank based multicarrier modulation for wireless communications," *EURASIP J. Appl. Signal Process.*, vol. 2007, 2007, Art. no. 049389.
[15] D. Waldhauser, L. Baltar, and J. Nossek, "MMSE subcarrier equalization for filter bank based multicarrier systems," in *Proc. IEEE 9th Workshop Signal Process. Adv. Wireless Commun.*, 2008, pp. 525–529.

[16] X. Mestre, M. Majoral, and S. Pfletschinger, "An asymptotic approach to parallel equalization of filter bank based multicarrier signals," *IEEE Trans. Signal Process.*, vol. 61, no. 14, pp. 3592–3606, Jul. 2013.
[17] M. Bellanger, "FS-FBMC: An alternative scheme for filter bank based multicarrier transmission," in *Proc. 2012 5th Int. Symp. Commun., Control Signal Process.*, May 2012, pp. 1–4.
[18] D. Mattera, M. Tanda, and M. Bellanger, "Frequency-spreading implementation of OFDM/OQAM systems," in *Proc. 2012 Int. Symp. Wireless Commun. Syst.*, Aug. 2012, pp. 176–180.
[19] M. Renfors, J. Yli-Kaakinen, and F. J. Harris, "Analysis and design of efficient and flexible fast-convolution based multirate filter banks," *IEEE Trans. Signal Process.*, vol. 62, no. 15, pp. 3768–3783, Aug. 2014.
[20] P. Duhamel and M. Vetterli, "Fast fourier transforms: A tutorial review and a state of the art," *Signal Process.*, vol. 19, no. 4, pp. 259–299, 1990.
[21] R. J. Essiambre, G. Kramer, P. J. Winzer, G. J. Foschini, and B. Goebel, "Capacity limits of optical fiber networks," *J. Lightw. Technol.*, vol. 28, no. 4, pp. 662–701, Feb. 2010.
[22] T. Mizuochi, "Recent progress in forward error correction and its interplay with transmission impairments," *IEEE J. Sel. Topics Quantum Electron.*, vol. 12, no. 4, pp. 544–554, Jul. 2006.